

Lawrence Berkeley National Laboratory

Lawrence Berkeley National Laboratory

Title

Localization of metal-induced gap states at the metal-insulator interface: Origin of flux noise in SQUIDs and superconducting qubits

Permalink

<https://escholarship.org/uc/item/70r9r4qd>

Author

Choi, SangKook

Publication Date

2009-11-03

Peer reviewed

Localization of Metal-Induced Gap States at the Metal-Insulator Interface: Origin of Flux Noise in SQUIDs and Superconducting Qubits

SangKook Choi, Dung-Hai Lee, Steven G. Louie, and John Clarke

Department of Physics, University of California, Berkeley
and
Materials Sciences Division, Lawrence Berkeley National Laboratory

The origin of magnetic flux noise in Superconducting Quantum Interference Devices with a power spectrum scaling as $1/f$ (f is frequency) has been a puzzle for over 20 years. This noise limits the decoherence time of superconducting qubits. A consensus has emerged that the noise arises from fluctuating spins of localized electrons with an areal density of $5 \times 10^{17} \text{ m}^{-2}$. We show that, in the presence of potential disorder at the metal-insulator interface, some of the metal-induced gap states become localized and produce local moments. A modest level of disorder yields the observed areal density.

Well below 1 K, low-transition temperature Superconducting Quantum Interference Devices [1] (SQUIDs) exhibit magnetic flux noise [2] with a temperature-independent spectral density scaling as $1/f^\alpha$, where f is frequency and $0.6 \leq \alpha \leq 1$. The noise magnitude, a few $\mu\Phi_0\text{Hz}^{-1/2}$ at 1 Hz (Φ_0 is the flux quantum), scales slowly with the SQUID area, and does not depend significantly on the nature of the thin film superconductor or the substrate on which it is deposited. The substrate is typically silicon or sapphire, which are insulators at low temperatures [2]. Flux noise of similar magnitude is observed in flux [3,4] and phase [5] qubits. Flux noise limits the decoherence time of superconducting, flux sensitive qubits making scale-up for quantum computing problematic. The near-insensitivity of noise magnitude to device area [2,5,6] suggests the origin of the noise is local. Koch *et al.* [7] proposed a model in which electrons hop stochastically between traps with different preferential spin orientations. A broad distribution of time constants is necessary to produce a $1/f$ power spectrum [8,9]. They found that the major noise contribution arises from electrons above and below the superconducting loop of the SQUID or qubit [5,7], and that an areal density of about $5 \times 10^{17} \text{ m}^{-2}$ unpaired spins is required to account for the observed noise magnitude. De Sousa [10] proposed that the noise arises from spin flips of paramagnetic dangling bonds at the Si-SiO₂ interface. Assuming an array of localized electrons, Faoro and Ioffe [11] suggested that the noise results from electron spin diffusion. Sendelbach *et al.* [12] showed that thin-film SQUIDs are paramagnetic, with a Curie ($1/T$) susceptibility (T is temperature). Assuming the paramagnetic moments arise from localized electrons, they deduced an areal density of $5 \times 10^{17} \text{ m}^{-2}$. Subsequently, Bluhm *et al.* [13] used a scanning SQUID microscope to measure the low-temperature paramagnetic response of

(nonsuperconducting) Au rings deposited on Si substrates, and reported an areal density of $4 \times 10^{17} \text{ m}^{-2}$ for localized electrons. Paramagnetism was not observed on the bare Si substrate.

In this Letter we propose that the local magnetic moments originate in metal-induced gap states (MIGS) [14] localized by potential disorder at the metal-insulator interface. At an ideal interface, MIGS are states in the band gap that are evanescent in the insulator and extended in the metal [14] (Fig.1). In reality, at a nonepitaxial metal-insulator interface there are inevitably random fluctuations in the electronic potential. The MIGS are particularly sensitive to these potential fluctuations, and a significant fraction of them-with single occupancy-becomes strongly localized near the interface, producing the observed paramagnetic spins. Fluctuations [15] of these local moments yield temperature-independent $1/f$ flux noise.

To illustrate the effects of potential fluctuations on the MIGS we start with a tight-binding model for the metal-insulator interface, consisting of the (100) face of a simple-cubic metal epitaxially joined to the (100) face of an insulator in a CsCl structure (Fig. 2(a)). For the metal we assume a single s-orbital per unit cell and nearest neighbor (NN) hopping. For the insulator we place an s-orbital on each of the two basis sites of the CsCl structure and assume both NN and next-nearest neighbor (NNN) hopping. The parameters are chosen so that the metal s-orbitals are at zero energy and connected by a NN hopping energy of -0.83 eV. The onsite energy of the orbitals on the Cs and Cl sites is taken to be -4 eV and 2 eV, respectively, and both the NN and NNN hopping energies are set to -0.5 eV. These parameters yield a band width of 10 eV for the metal, and 8 and 4 eV band widths, respectively, for the valence and conduction bands of the insulator

with a band gap of 2 eV (Fig. 2(d)). These band structure values are typical for conventional metals and for semiconductors and insulators. For the interface we take the hopping energy between the metallic and insulating atoms closest to the interface to be -0.67 eV, the arithmetic mean of -0.83 and -0.5 eV.

The electronic structure of the ideal metal-insulator junction is calculated using a supercell [16] containing $20 \times 20 \times 20$ metal unit cells and $20 \times 20 \times 20$ insulator unit cells, a total of 24,000 atoms. The total density of states (DOS) of the supercell (Fig. 2(e)) shows a nearly flat DOS in the band gap region. The states in the insulator band gap are MIGS that are extended in the metal, decaying rapidly away from the interface into the insulator. Our model with a lattice constant of 0.15 nm yields an areal density of states for the MIGS of about $3 \times 10^{18} \text{ eV}^{-1} \text{ m}^{-2}$, consistent with earlier self-consistent pseudopotential calculations [17].

To mimic the effects of interfacial randomness, we allow the onsite energy to fluctuate for both metal and insulator atoms near the interface [18]. Specifically we assume an energy distribution $P(E) = (2\pi)^{-1/2} \delta^{-1} \exp[-(E - E_0)^2/2\delta^2]$, where E_0 is the original onsite energy without disorder, and δ is the standard deviation. We characterize the degree of disorder by the dimensionless ratio $R = 2\delta/W$, where W is the bandwidth of the metal. For those MIGS that become localized, the energy cost, U_i , for double occupation is large, and we cannot use a noninteracting electron approach. Instead we adopt a strategy similar to that used by Anderson in his calculation of local moment formation [19]. We separate the space near the interface into 3 regions: (i) the perfect metal region (M), (ii) an interfacial region consisting of 2 layers of metal unit cells and 2

layers of insulator unit cells (D) (Fig. 2(b)), and (iii) the perfect insulator region (I). Region (ii) is analogous to the impurity in Anderson's analysis.

We first compute the single-particle eigenstates $\varphi_i(\mathbf{r})$ of region D *in isolation*. For each of these states, we compute U_i (using a long-range Coulomb potential with an onsite cutoff of 10 eV) and the hybridization energy Γ_i due to hopping to the metal and the insulator [20]. With the computed values of U_i and Γ_i , we solve Anderson's equation for the spin-dependent occupation for each localized state $|i\rangle$:

$$\langle n_{i,\sigma} \rangle = \frac{1}{\pi} \int_{-\infty}^{E_F} dE' \frac{\Gamma_i}{(E' - E_{i,\sigma})^2 + \Gamma_i^2} . \quad (1)$$

Here, $E_{i,\sigma} = E_i + U_i \langle n_{i,-\sigma} \rangle$ and σ is the spin index. The net moment associated with the state is given by $m_i = \mu_B \langle n_{i,\sigma} \rangle - \langle n_{i,-\sigma} \rangle$. Equation (1) and the associated expression for the net moment of the localized states are calculated within the self-consistent Hartree-Fock approximation [19]. An $m_i \neq 0$ solution is obtained only when $U_i/(E_F - E_i)$ exceeds a critical value which depends on $\Gamma_i/(E_F - E_i)$. In the large U_i limit, it is more appropriate to start from the weak coupling limit ($\Gamma_i=0$), where the localized state is populated by a single electron, and treat Γ_i as a perturbation. By calculating the areal density of such moment-bearing localized states we obtain an estimate of the density of spin-1/2 local moments.

Figure 3 shows the calculated distribution $\rho(E, U)$ in the isolated interfacial region for $R= 0.05, 0.1, 0.15, 0.2, 0.25,$ and 0.3 ; for each value, higher values of U correspond to

more localized states. As expected we see that, for any given degree of randomness, the states with energy inside the insulator band gap (the MIGS) or those at the band edges are most susceptible to localization. Figure 4 shows a perspective plot of the charge density of two states, with high and low values of U_i , showing the correlation between the degree of wavefunction localization and the value of U_i . Both states are centered in the insulator, a general characteristic of localized states in the band gap originating from the MIGS.

Setting the Fermi energy at the insulator midgap value, we estimate the areal density of spins for a given degree of randomness R . The top panel in Fig. 5 depicts the distribution $\rho(E, m)$ of the spin moments as a function of energy. We see that for small R virtually all the local moments are derived from the MIGS. The bottom panel of Fig. 5 shows the calculated areal density of local moments versus R . Our simple model thus indicates that moderate potential fluctuations ($R \sim 0.15 - 0.2$) at the interface produce an areal density of localized moments comparable to experimental values [21]. Although our analysis is for a specific model, we expect the general physical picture to remain valid for real materials. First, the formation of MIGS at a metal-insulator interface is universal, and their areal density is rather insensitive to the nature of the materials as discussed in EPAPS [20] and shown numerically in Ref. [17]. Second, the formation of local moments from the combination of localized states and Coulomb interaction is a general phenomenon [19]. We also note that our analysis should not be significantly modified when the metal is superconducting. This is because the U_i for the localized states is generally much greater than the pairing gap. Of course, extended states with negligible U_i would be paired.

Given our picture of the origin of the localized spin-1/2 moments, how do they produce $1/f$ flux noise with a spectral density $S_{\Phi}(f) \propto 1/f^{\alpha}$? The local moments interact via mechanisms such as direct superexchange and the RKKY interaction[11,22-24] between themselves, and Kondo exchange with the quasiparticles in the superconductor. The above system can exhibit a spin-glass transition [25], which could account for the observed susceptibility cusp [12] near 55 mK. At temperatures higher than 55mK, however, experiments suggest that the spins are in thermal equilibrium [26] and exhibit a $1/T$ (Curie Law) static susceptibility [12,13]. In this temperature regime, for $hf \ll k_B T$ standard linear response theory [27] shows that the imaginary part of the dynamical susceptibility $\chi''(f, T) = A(f, T)(hf/k_B T)$. Here, $A(f, T) \propto \sum_{\mu} \sum_{\alpha, \beta} P_{\alpha} \delta(hf + E_{\alpha} - E_{\beta}) |\langle \beta | S_{\mu} | \alpha \rangle|^2$, where S_{μ} is the μ -th component of the spin operator, α and β label the exact eigenstates, and P_{α} is the Boltzmann distribution associated with state α . Combining the above result with the fluctuation-dissipation theorem [15] which relates the flux noise to $\chi''(f, T)$, namely $S_{\Phi}(f, T) \propto k_B T \chi''(f, T) / hf$, we conclude that the observed $1/f^{\alpha}$ spectral density implies $A(f, T) \propto 1/f^{\alpha}$ ($0.6 \leq \alpha \leq 1$). Assuming low frequency contributions dominate the Kramers-Kronig transform, this result is consistent with the observed $1/T$ static susceptibility, and the recent measurement [28] showing that flux noise in a SQUID is highly correlated with fluctuations in its inductance. However, without knowing the form of the interaction between the spins, one cannot derive this behavior for $A(f, T)$ theoretically.

In conclusion, we have presented a theory for the origin of the localized magnetic moments which have been shown experimentally to give rise to the ubiquitous low temperature flux $1/f$ noise observed in SQUIDs and superconducting qubits. In particular

we have shown that for a *generic* metal-insulator interface, disorder localizes a substantial fraction of the metal-induced gap states (MIGs), causing them to bear local moments. Although MIGs have been known to exist at metal-insulator interfaces for three decades, we believe this is the first understanding of their nature in the presence of strong local correlation and disorder. Provided the temperature is above any possible spin glass transition, experiments show that fluctuations of these local moments produce a paramagnetic χ' and a power-law, frequency-dependent χ'' which in turn leads to flux $1/f$ noise. It is important to realize that localized MIGS occur not only at the metal-substrate interface but also at the interface between the metal and the oxide that inevitably forms on the surface of superconducting films such as aluminum and niobium. There are a number of open problems, for example, the precise interaction between the local moments, its relation to the value of α , and the possibility of a spin glass phase at low temperatures. A particular intriguing experimental issue to address is why different metals and substrates evidently have such similar values of R , around 0.15. From an experimental point of view, to improve the performance of SQUIDs and superconducting qubits we need to understand how to control and reduce the disorder at metal-insulator interfaces, for example, by growing the superconductor epitaxially on its substrate.

We thank Robert McDermott and Kam Moler for prepublication copies of their papers. S.C. and S.G.L. thanks Manish Jain and Jay D. Sau for fruitful discussions. This work was supported by the Director, Office of Science, Office of Basic Energy Sciences, Materials Science and Engineering Division, of the U.S. Department of Energy under Contract No. DE-AC02-05CH11231. S.C. acknowledges support from a Samsung Graduate Fellowship.

References

- [1] J.Clarke and A.I.Braginski, *The SQUID Handbook* (Wiley-VCH, GmbH and Weinheim, 2004), Vol. 1.
- [2] F.C.Wellstood, C.Urbina, and J.Clarke, *Appl. Phys. Lett.* **50**, 772 (1987).
- [3] F.Yoshihara, K.Harrabi, A.O.Niskanen, Y.Nakamura, and J.S.Tsai, *Phys. Rev. Lett.* **97**, 167001 (2006).
- [4] K.Kakuyanagi *et al.*, *Phys. Rev. Lett.* **98**, 047004 (2007).
- [5] R.C.Bialczak *et al.*, *Phys. Rev. Lett.* **99**, 187006 (2007).
- [6] T.Lanting *et al.*, *Phys. Rev. B* **79**, 060509(R) (2009).
- [7] R.H.Koch, D.P.DiVincenzo, and J.Clarke, *Phys. Rev. Lett.* **98**, 267003 (2007).
- [8] S.J.Machlup, *J. Appl. Phys.* **25**, 341 (1954).
- [9] P.Dutta and P.M.Horn, *Rev. Mod. Phys.* **53**, 497 (1981).
- [10] R.de Sousa, *Phys. Rev. B* **76**, 245306 (2007).
- [11] L.Faoro and L.B.Ioffe, *Phys. Rev. Lett.* **100**, 227005 (2008).
- [12] S.Sendelbach *et al.*, *Phys. Rev. Lett.* **100**, 227006 (2008).
- [13] H.Blumh *et al.*, arXiv:cond-mat/0903.3748v1.
- [14] S.G.Louie and M.L.Cohen, *Phys. Rev. B* **13**, 2461 (1976).
- [15] H.Nyquist, *Phys. Rev.* **32**, 110 (1928).
- [16] M.L.Cohen, M.Schlüter, J.R.Chelikowsky, and S.G.Louie, *Phys. Rev. B* **12**, 5575 (1975).
- [17] S.G.Louie, J.R.Chelikowsky, and M.L.Cohen, *Phys. Rev. B* **15**, 2154 (1977).
- [18] P.W.Anderson, *Phys. Rev.* **109**, 1492 (1958).

- [19] P.W.Anderson, Phys. Rev. **124**, 41 (1975).
- [20] See EPAPS. For more information on EPAPS, see <http://www.aip.org/pubservs/epaps.html>.
- [21] If one includes the effect of metallic screening from region M on U_i (Ref. [29]), U_i would decrease by a factor of roughly 2 since the localized state in region I is located on average ~ 3 unit cell layers from region M. We estimate this effect reduces the spin density by $\sim 50\%$ at each R value, resulting in an areal density of $\sim 5 \times 10^{17} \text{m}^{-2}$ at $R \approx 0.15 - 0.2$.
- [22] M.A.Ruderman and C.Kittel, Phys. Rev. **96**, 99 (1954).
- [23] T.Kasuya, Prog. Theor. Phys. **16**, 45 (1956).
- [24] K.Yosida, Phys. Rev. **106**, 893 (1957).
- [25] M.B.Weissman, Rev. Mod. Phys. **65**, 829 (1993).
- [26] R.Harris *et al.*, Phys. Rev. Lett. **101**, 117003 (2008).
- [27] A.L.Fetter and J.D.Walecka, *Quantum Theory of Many-Particle Systems*, (McGraw-Hill, New York, 1971) p.298.
- [28] S.Sendelbach *et al.*, Complex inductance, excess noise and surface magnetism in dc SQUIDs. Preprint.
- [29] J.D.Sau *et al.*, Phys. Rev. Lett. **101**, 026804 (1975).

Figure

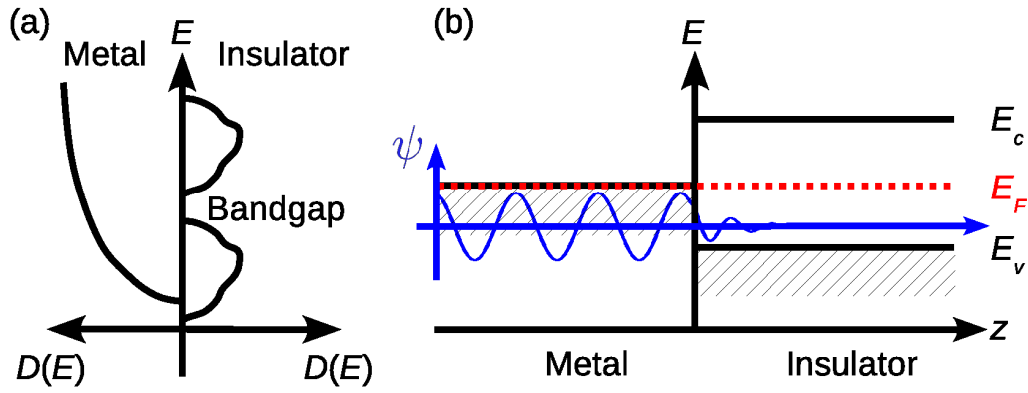


FIG. 1: (Color online) (a) Schematic density of states. (b) Metal-induced gap states (MIGS) at a perfect interface with energy in the band gap are extended in the metal and evanescent in the insulator.

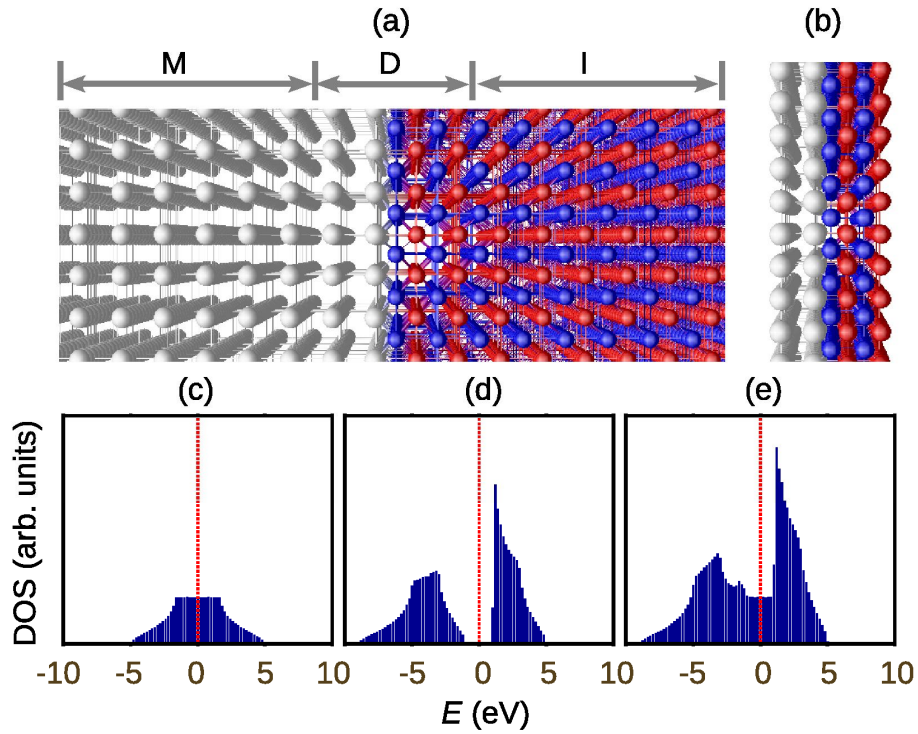


FIG. 2 : (Color online) (a) The metal (M) is assumed to have a simple cubic structure with one atom per unit cell and the insulator (I) a CsCl structure with two atoms per unit cell. (b) Interfacial region (D) consists of 2 layers of metal unit cells and 2 layers of insulator unit cells. The lattice constant is taken as 0.15 nm. Computed DOS with Fermi energy (dotted red line) set to zero. (c) Typical metal with 10 eV bandwidth. (d) Typical insulator with a 2 eV band gap separating two bands of about 8 eV and 4 eV. (e) Metal-insulator interface with MIGS in the band gap of the insulator produced by the presence of the metal.

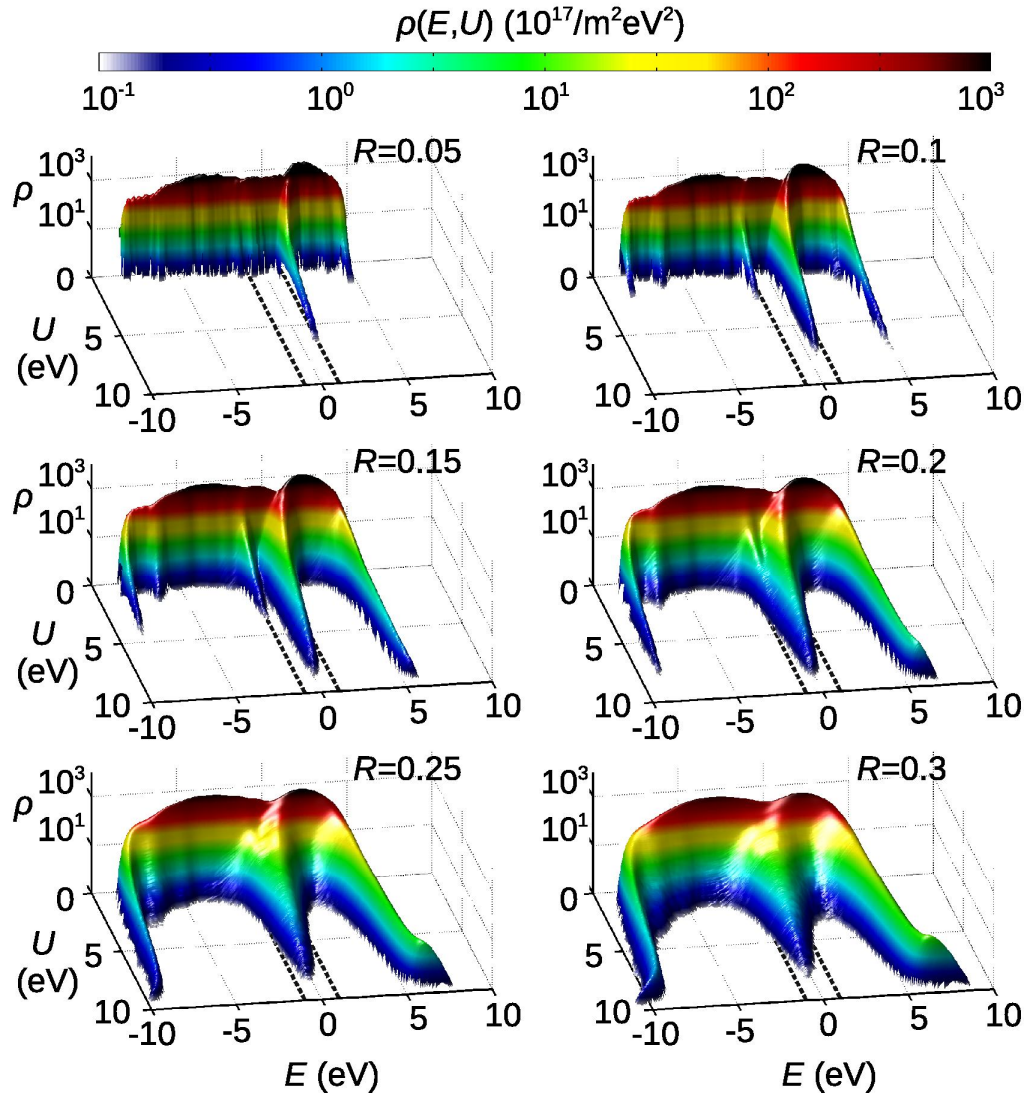


FIG. 3: (Color online) Density of states distribution $\rho(E,U)$ as a function of energy E and Hubbard energy U for 6 values of the randomness parameter R in the isolated D region of Fig. 2. For a given value of R , the highest values of U , resulting in the most highly localized states, appear in the band gap of insulator and at the edges of the bands. The position of the band gap of the insulator is represented by black dashed lines.

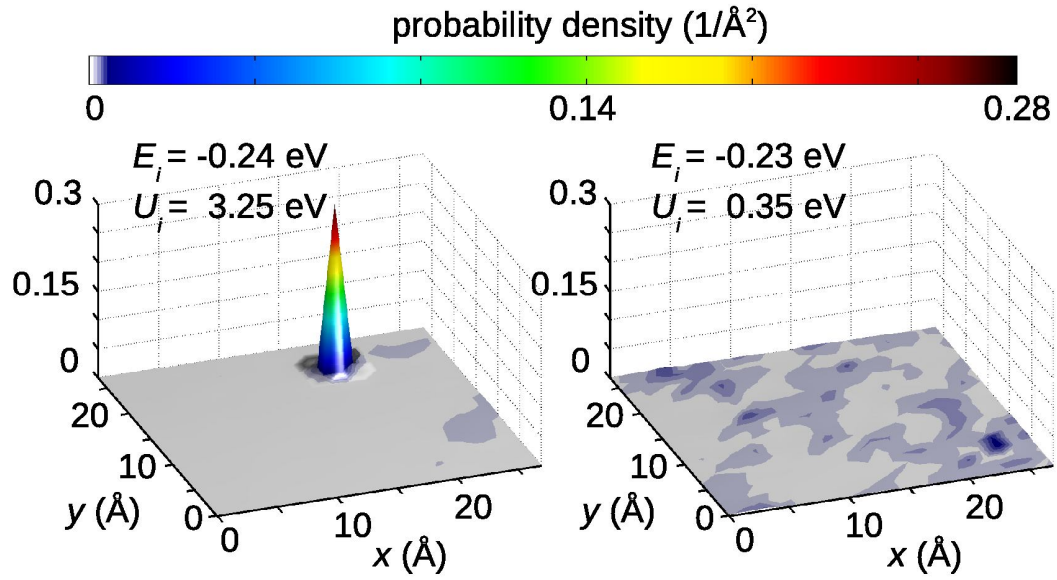


FIG. 4: (Color online) Perspective view images of the 2-dimensional probability density distribution at the interfacial region D along directions parallel to the interface (x- and y-directions), integrated along the z-direction. (a) States with $U_i=3.25$ eV and $E_i=-0.24$ eV and (b) with $U_i=0.35$ eV and $E_i=-0.23$ eV, respectively.

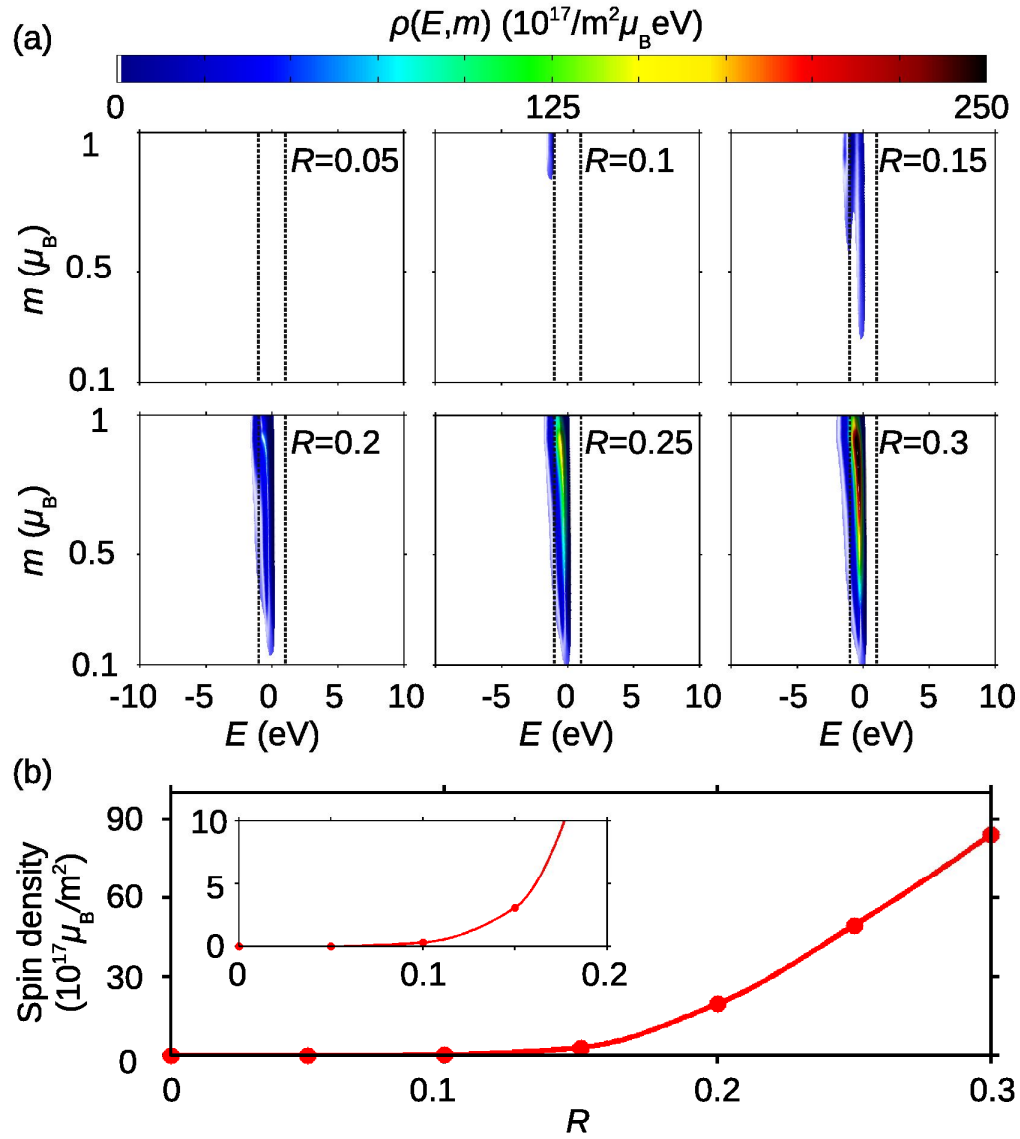


FIG. 5: (Color online) (a) Electron density distribution $\rho(E, m)$ as a function of electron energy E and spin moment m for 6 values of R . We simulated 5000 different configurations of disorder for each value of R . The position of the insulator band gap is represented by black dashed lines. Virtually all the magnetic moments are from the MIGS in the band gap of the insulator. (b) Integrated spin density versus randomness parameter R .

**Supplements to
“Localization of Metal-Induced Gap States at the Metal-Insulator
Interface: Origin of Flux Noise in SQUIDs and Superconducting
Qubits”**

SangKook Choi,^{1,2} Dung-Hai Lee,^{1,2} Steven G. Louie,^{1,2} and John Clarke^{1,2*}

¹Department of Physics, University of California at Berkeley, California 94720

²Materials Sciences Division, Lawrence Berkeley National Laboratory, Berkeley, California 94720

Areal density of MIGS. We give a simple estimate of the areal density of MIGS. In a two-band tight-binding model [1], the amplitude squared of the evanescent solutions [2] close to the valence band edge has an energy-dependent decay length $\beta(E) = 2[2m^*(E - E_{VBM})/\hbar^2]^{1/2}$, where m^* is the electron effective mass and E_{VBM} is the energy of the valence band maximum. Near the conduction band edge E_{CBM} , $\beta(E) = 2[2m^*(E_{CBM} - E)/\hbar^2]^{1/2}$. The areal density N of MIGS in the insulator (in units of states per unit area) is given by [3]

$$N = \int_0^{E_F} dE \int_0^\infty dz \eta(E) e^{-\beta(E)z} = \eta \int_0^{E_F} dE \frac{1}{\beta(E)}, \quad (2)$$

where we have assumed the density of states $\eta(E)$ of the metal to be constant over the energy range of the band gap. Inserting the expression for $\beta(E)$ into (2), we obtain

$$N = \eta [(\hbar^2/2m^*)(E_F - E_{VBM})]^{1/2}. \quad (3)$$

For most semiconductors and insulators [4], $m_e/m^* \approx 1 + C_1/E_g$ and $E_F - E_{VBM} = C_2 \times E_g$ with $C_1 \approx 10$ eV and $C_2 \approx 0.5$; furthermore, for most metals $\eta(E)$ is of the same order of magnitude. Consequently, the approximate expression

$$N \approx \eta [(\hbar^2/2m_e)C_1C_2]^{1/2} \quad (4)$$

is relatively insensitive to the nature of both the metal and the insulator. Using the typical values $\eta(E) \approx 2 \times 10^{28} \text{m}^{-3} \text{-eV}^{-1}$ and $C_1 C_2 \approx 5 \text{ eV}$, we obtain $N \approx 8 \times 10^{18} \text{ m}^{-2}$, in good agreement with pseudopotential calculation [5] for Al in contact with Si, GaAs or ZnS.

Hubbard energy U_i . We calculate the Hubbard energy U_i for double occupation for states $\varphi_i(\mathbf{r})$ in the isolated D region by evaluating the integral

$$U_i = \int_D d\mathbf{r} d\mathbf{r}' \frac{|\varphi_{i,\uparrow}(\mathbf{r})|^2 |\varphi_{i,\downarrow}(\mathbf{r}')|^2}{|\mathbf{r} - \mathbf{r}'|} \quad (5)$$

over the supercell. Within our tight-binding supercell scheme, two additional factors need to be included. (i) The part of the Coulomb integral on the same atomic site is replaced with the value of an onsite Hubbard U_0 . (ii) When the localization length (ξ) of the localized states is larger than the supercell size, there is overlap of wavefunctions from the neighboring supercell; this overestimates U_i for the very weakly localized states.

Given that the participation number, $P_i = 1 / \sum_j |\varphi_i(\mathbf{r}_j)|^4 \sim (\xi_i / a)^d$ in a disordered d -

dimensional system with supercell lattice constant a and $U_i \propto 1 / \xi_i$, we map the U_i value of the finite supercell onto that of an infinite supercell using a scaling law [6] for ξ .

Hybridization energy broadening Γ_i . The hybridization-energy broadening of the localized states arises from couplings to the extended states in the metal as well as those in the insulator, and is given by

$$\Gamma_i = \Gamma_i^M + \Gamma_i^I \quad (6)$$

$$\Gamma_i^M = \pi / V_i^M \int_{ave}^2 \rho^M(E), \quad \Gamma_i^I = \pi / V_i^I \int_{ave}^2 \rho^I(E), \quad (7)$$

where $\rho^{M(I)}(E)$ is the density of extended states in M (I) at the energy of the localized state E , and $V_i^{M(I)}$ is the hopping matrix element between an extended state in M (I) and a localized state in D (*ave* indicates averaging over the extended states). Extended eigenstates in M(I) are a linear combination of constituent orbitals; the $V_i^{M(I)}$ can then be expressed in terms of the coupling of these orbitals to those in D. For example, the localized states inside the band gap of the insulator are hybridized with only extended states in M, and $\Gamma_i = \Gamma_i^M \approx \pi V^2 d_i / W$. (Here d_i is the charge of the localized state $|i\rangle$ in the unit cell layer immediately adjacent to M.)

[1] J.K.Tomfohr and O.F.Sankey, *Phys. Rev. B* **65**, 245105 (2002).

[2] W.Kohn, *Phys. Rev.* **115**, 809 (1959).

[3] S.G.Louie and M.L.Cohen, *Phys. Rev. B* **13**, 2461 (1976).

[4] P.Y.Yu and M.Cardona. *Fundamentals of Semiconductors: Physics and Materials Properties* (Springer, Berlin, 2005).

[5] S.G.Louie, J.R.Chelikowsky, and M.L.Cohen, *Phys. Rev. B* **15**, 2154 (1977).

[6] A.MacKinnon and B.Kramer, *Phys. Rev. Lett.* **47**, 1546 (1981).

* Electronic address: jclarke@berkeley.edu

DISCLAIMER

This document was prepared as an account of work sponsored by the United States Government. While this document is believed to contain correct information, neither the United States Government nor any agency thereof, nor The Regents of the University of California, nor any of their employees, makes any warranty, express or implied, or assumes any legal responsibility for the accuracy, completeness, or usefulness of any information, apparatus, product, or process disclosed, or represents that its use would not infringe privately owned rights. Reference herein to any specific commercial product, process, or service by its trade name, trademark, manufacturer, or otherwise, does not necessarily constitute or imply its endorsement, recommendation, or favoring by the United States Government or any agency thereof, or The Regents of the University of California. The views and opinions of authors expressed herein do not necessarily state or reflect those of the United States Government or any agency thereof or The Regents of the University of California.